Supplementary Figures

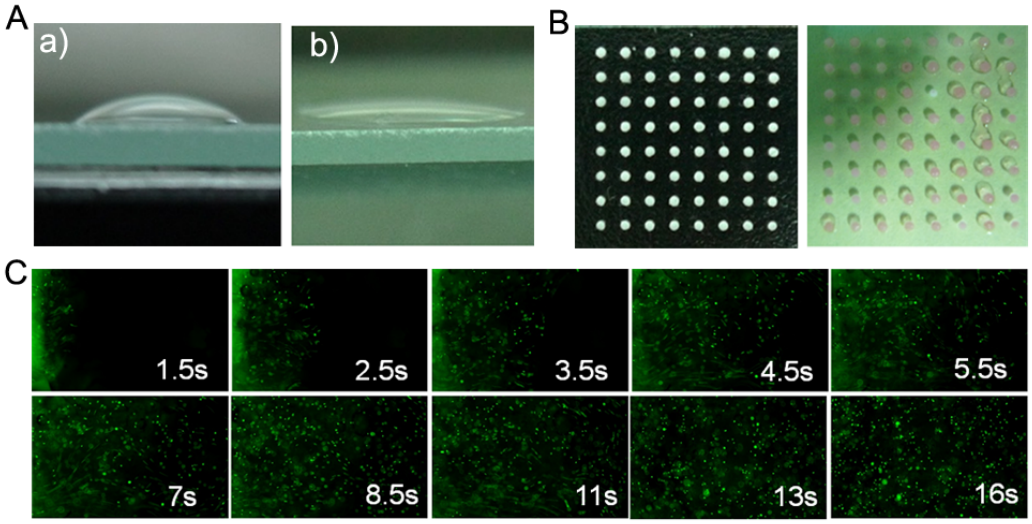

Fig. s1 A) Water drop on normal glass slide (a) and on plasma-treated hydrophilic glass slide (b). B) High-throughput auto-loading of phenol solution into microsponge pillar array by liquid-layer method. C) Dynamic absorbing process of fluorescent microbeads with dimeter of 10 μm into cell-laden microsponge by drop-wise pepitting method.

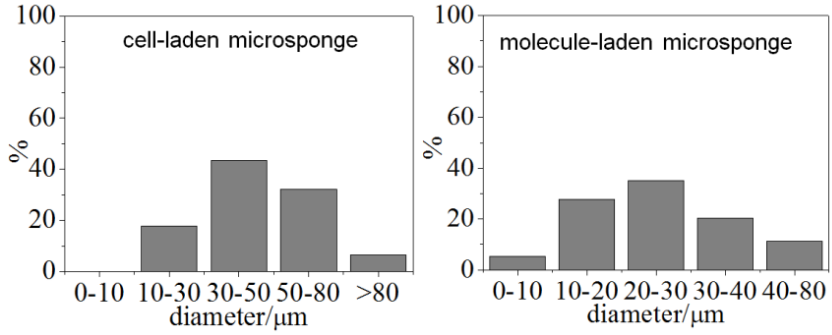

Fig. s2 Pore diameter distribution of cell-laden and molecule-laden microsponge.

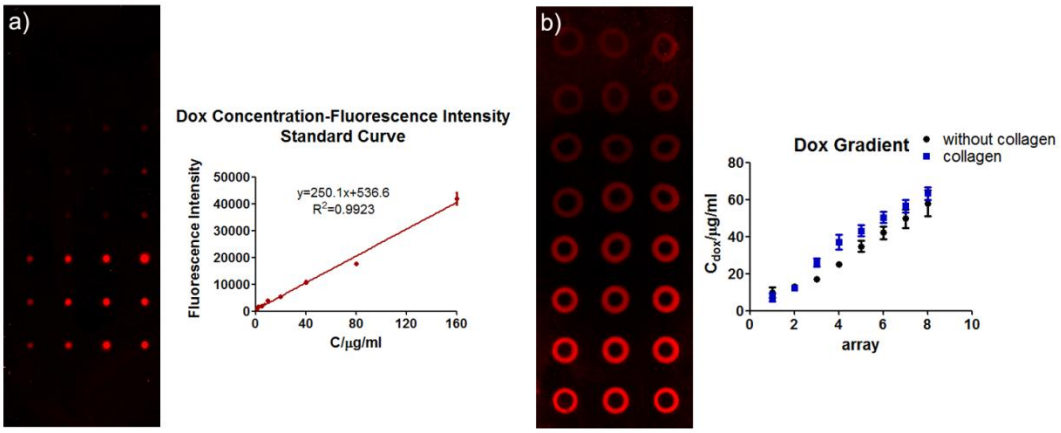

Fig. s3 a) Fluorescence image and quantified fluorescence instensities for establishing standard curve of fluorescence intensity change with different concentrations of Dox solution; b) Fluorescence image and concentration gradients of Dox in microsponge well array loaded with and without collagen gel, which showed

similar trend indicating no interference of collagen for Dox diffusion.

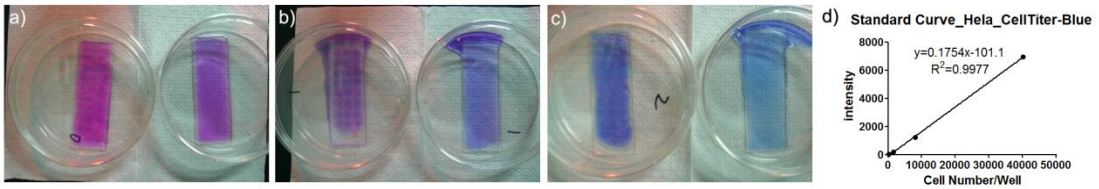

Fig. s4 Cell-Titer Blue assay for quantifying cell seeding efficiency via liquid-layer method with different initial cell seeding densities (a: 5×10^6 /ml, b: 1×10^6 /ml; c: 2×10^5/ml); d) Standard curve of cell number vs fluorescence intensity obtained with Cell-Titer Blue assay.

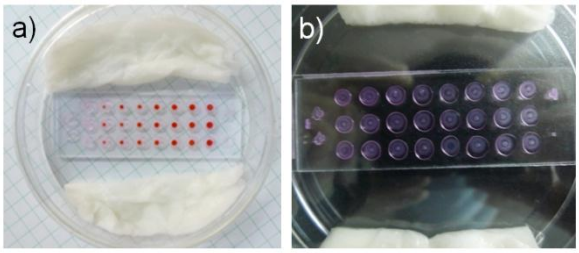

Fig. s5 The set-ups of drug cytotoxicity test (a) and tumor invasion assay (b).

Fig.s6 Vacuum packaging of microsponge chips for long term storage and shippment. Four microsponge chips were packaged in a vacuumed plastic bag by thermal-sealing.

Simulation of Dox diffusion

Equation of Species Transport in Porous Media were adopted with parameters listed in **Table 1**. As showed in **Table 2**, the concentration gradients of Dox obtained by simulation correlated well with both experimental results and theoretical calculation.

Equation of Species Transport in Porous Media

$$P_{1,j}\frac{\partial c_j}{\partial t} + P_{2,j} + \nabla \cdot \Gamma_j + u \cdot \nabla c_j = R_j + S_j \qquad (1)$$

$$P_{1,j} = \left(\varepsilon + \rho_b k_{p,j}\right) \qquad (2)$$

$$P_{2,j} = \left(c_j + c_{p,j}\rho_p\right)\frac{\partial \varepsilon}{\partial t}, \rho_p = \frac{\rho_b}{(1-\varepsilon)} \quad (3)$$

$$c_{p,j} = k_{p,j}c_j, k_{p,j} = \frac{\partial c_{p,j}}{\partial c} = \frac{\partial (k_{p,j}c_j)}{\partial c} \quad (4)$$

$$N_j = \Gamma_j + uc_j = -\left(D_{D,j} + D_{e,j}\right)\nabla c_j + uc_j \quad (5)$$

$$D_{e,j} = \varepsilon\tau_{F,j}D_{F,j} \quad (6)$$

Table 1 Parameters used in Model of Species Transport in Porous Media

PEGDA4000 density: ρ_p=1120 kg/m^3
microsponge height: h=0.3 mm
Doxorubicin molecular weight: M=543.52 g/mol
Doxorubicin diffusion coefficient: D_F=4e^{-10} m^2/s
Doxorubicin density concentration: c=64 μg/ml, 700μg/ml
Assuming no adsorption and dispersion, if the parameter is not an intermediate variable, it should be 0.
Velocity field: u=(0,0,0)m/s
Isotherm: k_p=0 m^3/kg
Dispersion tensor: D_D=0 m^2/s
Drug microsponge radius: R=0.3 mm, 0.42 mm, 0.6 mm, 0.74 mm, 0.85 mm, 0.95 mm, 1.04 mm, 1.13 mm
Drug microsponge porosity: ε=0.824
Drug microsponge Tortuosity: τ=4[1, 2]
Cell microsponge inner radius: Ri=1.2 mm, outer radius: Ro=1.7 mm
Cell microsponge porosity: ε=0.933
Cell microsponge Tortuosity: τ=2[1, 2]

Table 2 Diffusion concentration gradient of Dox obtained from theoretical calculation and COMSOL simulation

Array number		1	2	3	4	5	6	7	8
pillar radius /mm		0.3	0.42	0.6	0.74	0.85	0.95	1.04	1.13
Slide 1	Calculation	0.86	1.68	3.34	4.95	6.37	7.77	9.09	10.46
	Simulation	0.72	1.53	3.20	4.91	6.81	8.21	9.32	10.76
64μg/ml	Experiment	0.39	1.38	3.10	4.98	6.53	7.89	9.08	10.51
Slide 2	Calculation	9.51	18.40	36.55	54.12	69.68	84.93	99.40	114.41
	Simulation	8.24	18.14	35.94	51.58	73.96	91.68	104.74	118.63
700μg/ml	Experiment	13.33	28.62	35.45	55.00	77.62	89.56	99.43	114.14

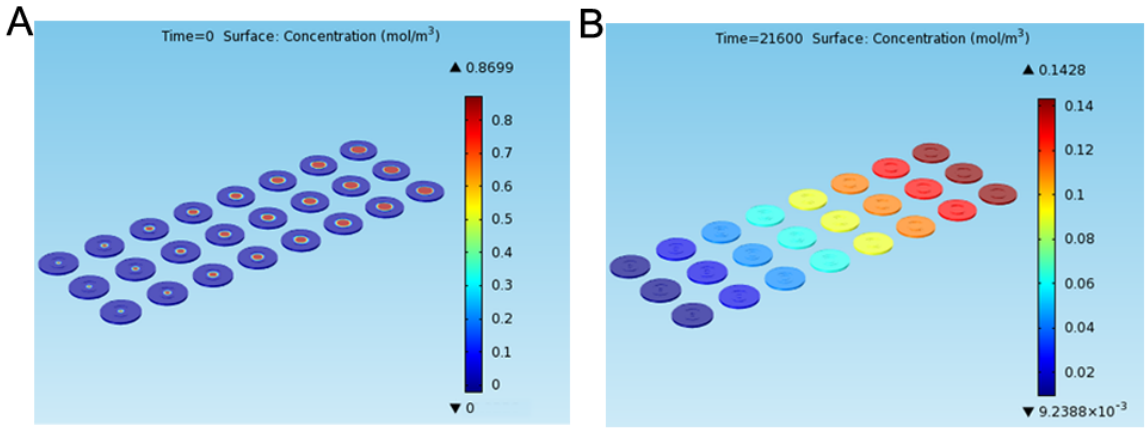

Fig. s7 Simulation of the dynamic formation of concentration discrete gradients by Dox diffusion (A-before; B-after) in the off-the-shelf microsponge array.

Supplemented Video:

Video 1

The autoloading process of 10μm fluorescence microbeads absorbed into a hexonal microsponge by drop-wising pipetting

Video 2

COMSOL simulation of the dynamic formation of concentration discrete gradients by Dox diffusion in the off-the-shelf microsponge array.

References

1 D. C. Scott, Pharm Res, 2001, 18, 1797-1800.

2 J. Lankelma, R. Fernandez Luque, H. Dekker, W. Schinkel and H. M. Pinedo, Microvasc Res, 2000, 59, 149-161.